EA-2 | 85

ASAT

Military Technical College
CAIRO - EGYPT

SHOCK WAVE BOUNDARY-LAYER INTERACTION IN GAS-PARTICLE FLOWS THROUGH DUCTS

K.A. IBRAHIM*

ABSTRACT

The problem of shock wave turbulent boundary-layer interaction in gas-particle flows through circular ducts is investigated experimentally. The effects of the amount of solids in the air flow, the intake design parameters such as; the upstream driving pressure, intake Mach number, duct length and the back pressure on the interaction characteristics have been investigated. The results indicate clearly that the interaction characteristics are mainly affected by the present of solid particles in the air flow and the duct length. A lower pressure recovery is expected as both of the intake Mach number and the amount of solid particles, suspended in the air, are increased. As the solids loading ratio increases the pressure recovery decreases, while as the duct length increases the shock interaction becomes stronger.

1. INTRODUCTION

The design and development of high performance turbomachinery operating in an ambient with solid particles requires a through knowledge of the fundamental phenomenon associated with particulate flows. Air craft engines and inductrial gas turbines operating in dusty areas or in places where the atmosphere is poluted by small particles can be examples of machines operating under gas-particle two phase flow conditions. The problem of shock wave boundary-layer interaction in cylinderical ducts is of great practical importance in the design of supersonic air intakes jet propulsion units, high speed centrifugal compressors and supersonic wind tunnels. Unlike the case of single phase flow, no experimental work has been published of shock wave boundary-layer interaction in a gas flow carrying particles through cylindrical ducts. Most of the recent studies in this field have been made on gas flow diffusers, nozzles and ducts operating when preceded by a normal shock boundary-layer interaction, [1-8].

In this paper, An experimental investigation of shock boundary-layer interaction in gas-solids flow cylindrical duct has been considered. Effects of interaction parameters such as; the upstream driving pressure, the intake Mach number, a duct length, and the back pressure as well as the

* Associate Professor, Mech. Eng. Dept., Menoufia University.

solids loading ratio on the pressure distribution caharcteristics of the interaction. In particular the variation of both the shock position inside the duct and the pressure recovery across the shock are examined, and consequently the intake design parameters can be optimized.

2. EXPERIMENTAL APPARATUS AND INSTRUMENTATION

The overall test rig layout is shown in Fig. 1. The rig comprises an air supply, a means of feeding the solid powder into the air flow, a test section, a means of separating the solids from the air flow and devices for air and solid flow measurements.

2.1 Air Supply

The air supply is from two air compressors with a free air delivery rating of 10 m^3/min at a pressure of 8 bar. The compressors deliver to an air receiver of 7.2 m^3 capacity, after being fully dried and filtered through a filter unit. The storage tank is connected to the rig by a pipeline 6.7 m long and 50.8 mm diameter .

2.2 Powder Feeding and Injection Systems

The solid material is stored in a hopper of 0.05 m^3 capacity which rests on a weighing machine. The space in the hopper above the powder is pressurized to assist the particle flow. The solid particles are introduced into the air flow through a combination of two valves. The lower valve is fitted with a pointer and a scale clibrated in 10^o intervals. This valve was used to control the solid flow rate over a wide range of values. The mixture is injected into a 2.54 cm pipe diameter and 30 cm length through four injectors mounted flush with the internal surface of the main pipe rig, Fig. 1. The injection system was found to provide a uniform steady flow of the mixture.

2.3 Solids Separation

After the air-solid suspension has passed through the test section, it is led into a cyclone-dump chamber designed to remove particles from the flow down to a diameter of 12.5 microns. The clean air flow; with unseparated particles; was passed from the top of the cyclone through a fabric bag filter and exhausted to atmosphere through a control valve. While the solid particles separated in the cyclone, were collected in the dump chamber. After a series of experimental runs, the powder has to be reloaded into the storage hopper for reuse.

2.4 Test Section

The test section is consists of a supersonic flow nozzle and a 25 mm diameter circular duct followed by a conical diffuser of inclined angle of 12^o and has an overall area ratio of 4:1. Two different nozzles were used and identified as follows:

The first nozzle has a throat radius of 10.02 mm, Ae/A^* = 1.556 and 1.9 exit Mach number. While the second nozzle has a throat radius of 10.81 mm, Ae/A^* = 1.337 and 1.7 exit Mach number. The nozzles were designed on an inviscid air flow basis, the discahrge Mach number of each was slightly modified from its design value. Thus for the desired discharge Mach numbers of 1.9 and 1.7, the nozzle Mach numbers were 2.15 and 1.8. Three

tested ducts, with different lengths (L/D = 20, 24 and 28), were used. On each duct length a series of static pressure tapping holes were drilled and spaced at intervals of 10 mm in the interaction region and 30 mm in the downstream region.

2.5 Measurements of Air and Solids Flow Rate

The air flow rate was measured by a standard orifice plate. The solids mass flow rate was measured by timing the change of weight of the solids hopper. A torque potentiometer was attached to the weighing machine pointer, Fig. 2, to provide an output voltage; which available to read from a digital voltameter. By this method and by the help of weighing machine calibration curve, the solids mass flow rate at any position of the valve opening was determined.

2.6 Pressure Measurements

The static pressure distribution along the duct wall was measured using a multiple U-tube manometer system. Two Bourdon pressure gages were used to measure the total intake pressure (P_o), before entering the test nozzle, and the downstream back pressure (P_B) in the diffuser tail pipe before the downstream valve.

3. RESULTS AND DISCUSSION

The experiments were carried out for a wide range of air flow rates and solids loading ratio. The solid particles used in these experiments were polyvinyle-cloride powders. The physical properties of this powder are shown in Table 1.

Table 1

Average particle size, Microns	Particle Density, Kg/m^3	Packed density, Kg/m^3	Specific heat $J/Kg.K^o$	Particle shape
150	1060	550	1340	almost perfect spheres

3.1 Pressure Distribution

A shock wave turbulent boundary-layer interaction in a gas-particle duct flow is governed by five design parameters; P_o, L , M_i, P_B and X. The effect of these parameters on the static pressure distribution is shown in Figs. 3-7. In such a flow system the inlet Mach number M_i is obtained by using a certain nozzle. The variation of the inlet boundary-layer thickness is achieved by varying the duct length at constant M_i and P_o. The boundary-layer just before the interaction also varies depending on the shock position within a constant duct length. This also could be achieved by varying the value of back pressure, P_B.

From Figs. 3 and 4, it can be seen that, for a certain nozzle-duct length combination and at a constant back pressure, the shock moves further as P_o or X increases. Also it is clear that as P_o or X increases the pressure gradient in the shock region decreases. This can be explained by noting that an increase of P_o moves the shock further into the duct giving the boundary-layer the chance to grow thicker resulting in a strong interaction, i.e. a weaker shock and smaller value of dP/dL are obtained. Also the persence of solid particles providing an additional pressure drop component through the mechanism of momentum exchange between the two phases and the additional turbulent energy will be produced in the flow. For these reasons, the maximum value of dP/dL occurs in pure air flow, X=0, and decreases with X increases. From Fig.5 , it can be seen that, for constant value of X and P_o, as the back pressure P_B increases; the following cases occur:

(1) the shock moves upstream and finally recedes into the nozzle, and (2) the shock strength increases and its interaction with the boundary-layer becomes weakness. Fig. 6, shows the variation of pressure along the duct length, for different duct lengths, while the remaining design parameters are kept constant. The results are for both air flow and suspension flow. From the results it can be seen that as the duct length increases, the shock moves further upstream and the value of dP/dL in the interaction region increases. The upstream movement of the shock is attributed to the increase in aerodynamic resistance of the longer duct. In the case of longer ducts the pressure continues to increase for a longer distance after the shock position. While for shorter ducts (for late shocks), the interaction completes rapidly. From these results it can be concluded that the best inlet conditions to the diffuser occur in the case of longer ducts and then a good diffuser performance will be obtained. Fig. 7, indicates the effect of changing the value of inlet flow Mach number M_i on the pressure distribution. For smaller value of M_i the interaction is stronger and the redistribution region is smaller. This is expected since the shock is moved further in the duct with the increase of M_i and this will give a thicker boundary-layer along the duct wall. Therefore, the length of redistribution region increases for the higher M_i.

3.2 Interaction Characteristics

The parameters describing the interaction characteristics (Xs and c_p) are defined in Fig.2. The shock position (Xs) is defined as the distance from the duct inlet to the point where the pressure distribution starts curving upwards. While the pressure recovery coefficient c_p is defined as;

$$C_p = \frac{(P_{max}/P_o) - (P_i/P_o)}{1 - (P_i/P_o)}$$

Referring to Fig. 2. and according to the above definition, Xs and C_p are obtained directly from the measurements of pressure distribution. The effects of X, P_o, P_B and L/D are quite clear in Figs. 8-11. Generally the value of C_p decreases with the increase of P_o and X, while it decreases with the increase of P_B and L/D. This is attributed to the fact that for the longer duct the shock interaction tends to start earlier,

6

while the boundary layer is still thin and the weak interaction with the thin boundary-layer occurs; i.e. higher pressure recovery occurs. For the case of small value of P_B the shock moves to the downstream where the boundary-layer is thicker and then C_p decreases. Also from Figs. 8-11 it can be seen that the shock moves further (Xs increases) inside the duct when the solids loading ratio X and P_o are increased or when P_B and L/D are decreased. In Figs. 9 and 11, the results for pure air flow are also illustrated for comparison with those for suspension flow. The values of Xs and C_p, for all tested duct lengths (L/D) and P_o, are mainly affected by the presence of solid particles in air flow.

4. CONCLUSION

The phenomenon of shock wave boundary layer interaction in a gas-solid flow duct has been studied experimentally. The results demonstrate that the pressure recovery coefficient and the shock position are mainly depend on the value of solids loading ratio, upstream driving pressure, back pressure, intake Mach number and the duct length. As the solids loading ratio increases the shock moves further downstream and the value of pressure recovery in the interaction region decreases. For a certain value of solids loading, the best inlet conditions to the diffuser occur in the case of longer duct. Also the pressure recovery coefficient has a higher value in the case of longer duct. This will give a good performance of diffuser. Therefore, in practice the longer ducts are recomended to be used especially in dusty areas.

REFERENCES

1. Livesey, J.L., and Odukwe, A.O., "Some Effects On Conical Diffuser Performance Of Preceding Normal Shock Boundary-Layer Interaction", Proc.Instn. Mech. Engrs., Vol. 188, 607-613 (1974).
2. Livesey, J.L., and Kamal, W.A., "Prediction of Diffuser Flow and Performance following a normal shock turbulent boundary-layer Interaction", Proceeding of the Symposium On Turbulent Shear Flow, PP. 12.1-12.10, Pennsylvania state Univ. (1977).
3. Arens, M., and Spiegler, E., "Shock-induced Boundary layer separation in over-expanded conical exhaust Nozzles", AIAA J, vol. 1, P. 578 (1963).
4. George, G., Brosh, A. and Vigas, J.R., "A Normal Sshock Wave Turbulent Boundary layer Interactions At Transonic Speeds", AIAA J. No. 76 P. 161 (1976).
5. Reda, C.C., and Murphy, J.D., "Shock Wave Turbulent Boundary Layer Interaction In Rectangular Channels", AIAA J., Vol 11, No.10, (1973).
6. Waltrup, P.J. and Billing,F., "Structure of Shock In Cylindrical Ducts", AIAA J., vol. 11, pp 1404-1408 (1973).
7. Fukuda, M.K., Hingst, W.R., and Reshotko, E., "Bleed Effect on Shock Boundary Layer Interaction In Supersonic Mixed Compression Inlet", Aircraft, J.,Vol. 4, No.2, (1977).
8. Kamal, W.A., WAHBA, E.M., and SABRY, T.I., "Shock wave-Boundary Layer Interaction In Cylindrical Ducts", 4th international conference for Mechanical Power Eng., Cairo Univ., paper V-29 (1982)

NOMENCLATURE

C_p Pressure recovery coefficient.
D_p Duct diameter
L Duct Length

M_i	Air Mach number at duct inlet
P^i	Static pressure
P_B	Back pressure
P_i	Static Pressure at duct inlet
P^o	Upstream driving pressure
X^{max}	Duct Maxmumim Static pressure
x	Solids loading ratio
Xs	Distance along the duct length
	Shock position

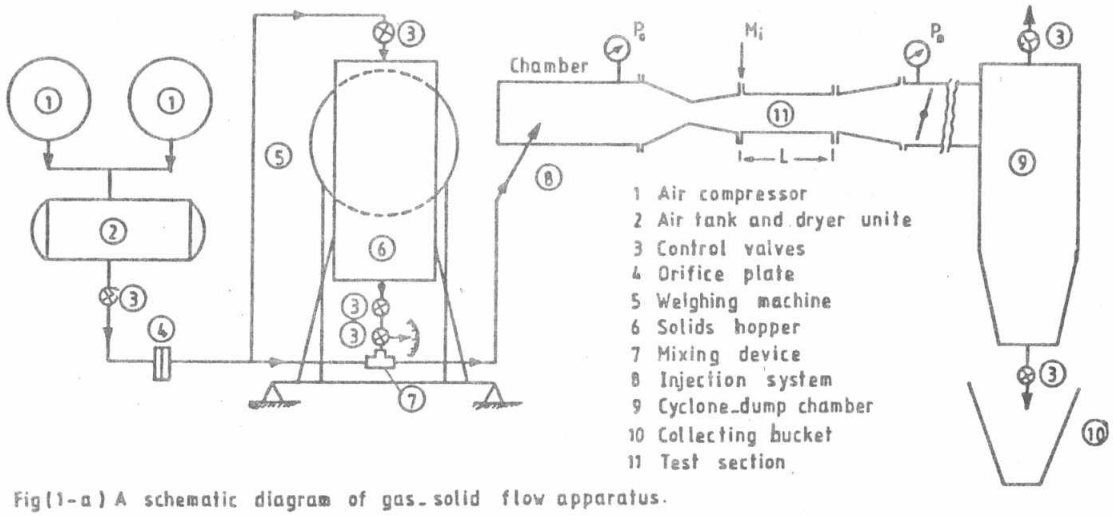

Fig(1-a) A schematic diagram of gas_solid flow apparatus.

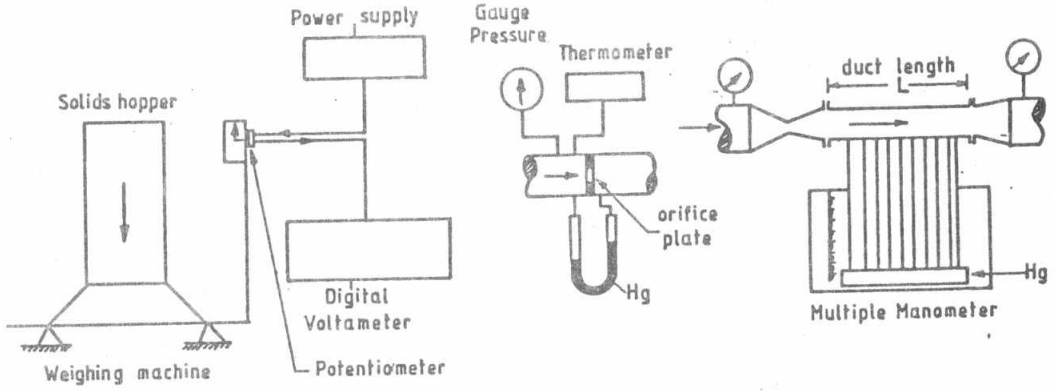

Fig(1-b) Schematic Diagram of the Instrumentation

6

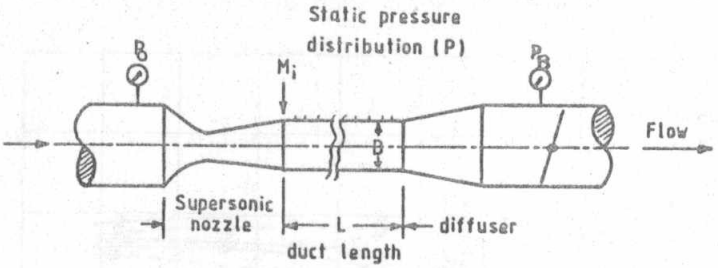

a) Shock boundary layer interaction parameter

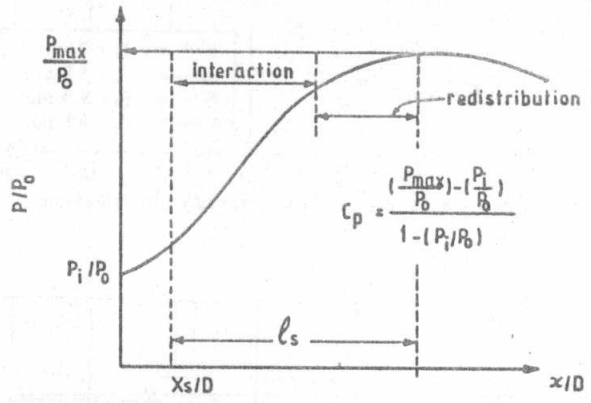

b) Interaction characterstics (Cp, Xs)

Fig (2) Shock wave boundary layer Interaction.

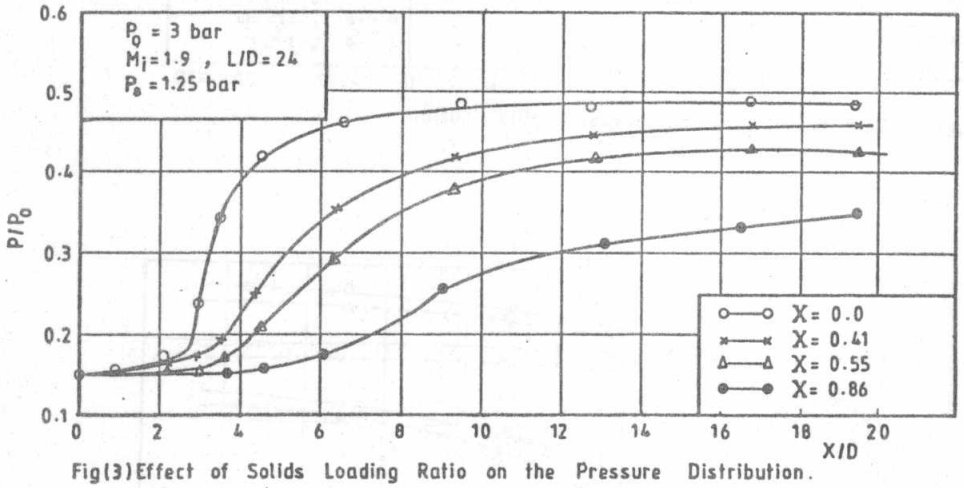

Fig(3) Effect of Solids Loading Ratio on the Pressure Distribution.

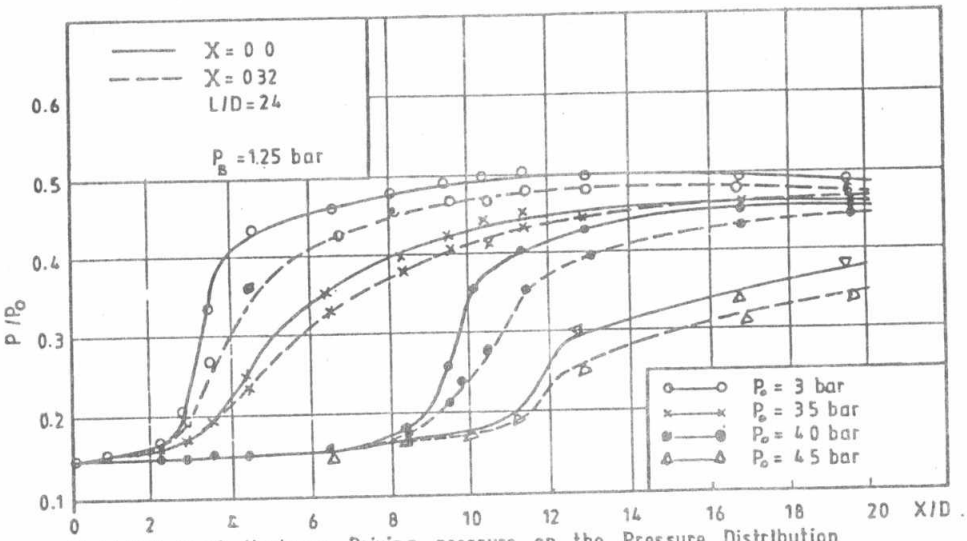

Fig(4) Effect of Upstream Driving pressure on the Pressure Distribution

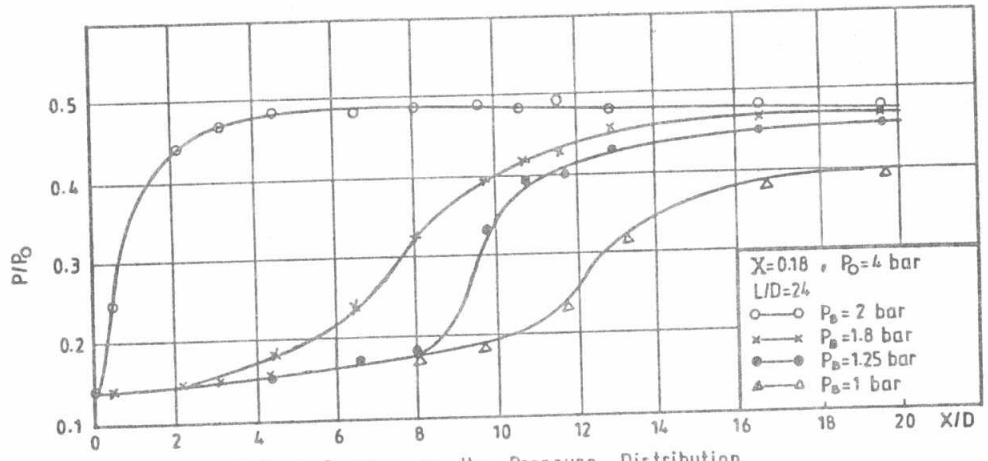

Fig(5) Effect of Back Pressure on the Pressure Distribution

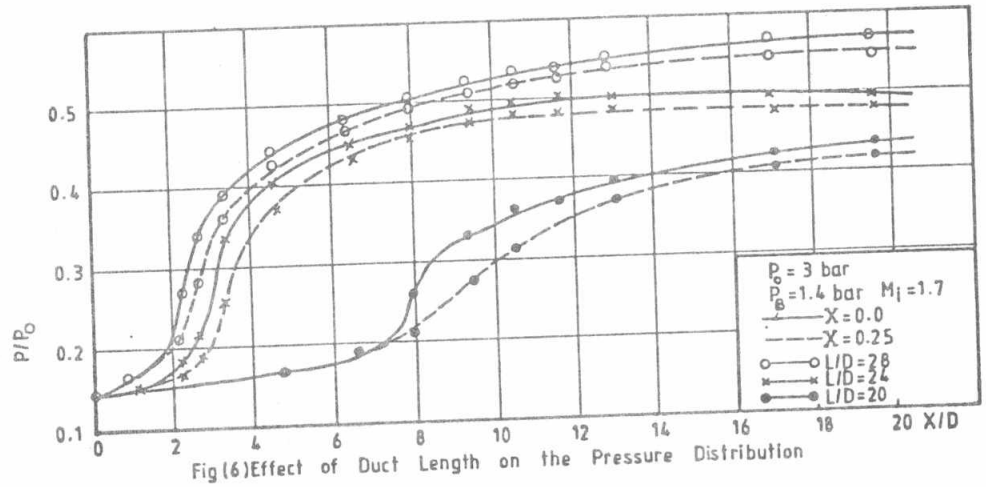

Fig(6) Effect of Duct Length on the Pressure Distribution

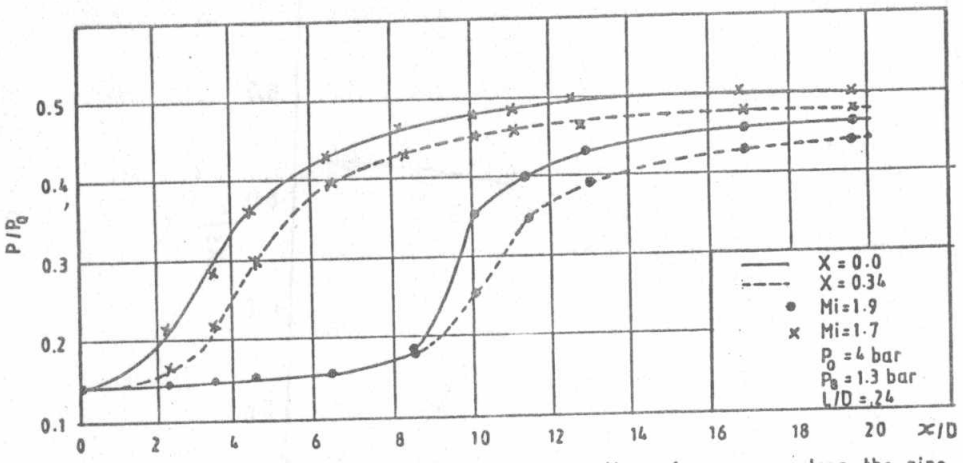

Fig(7) Effect of intake Mach number on the variation of pressure along the pipe.

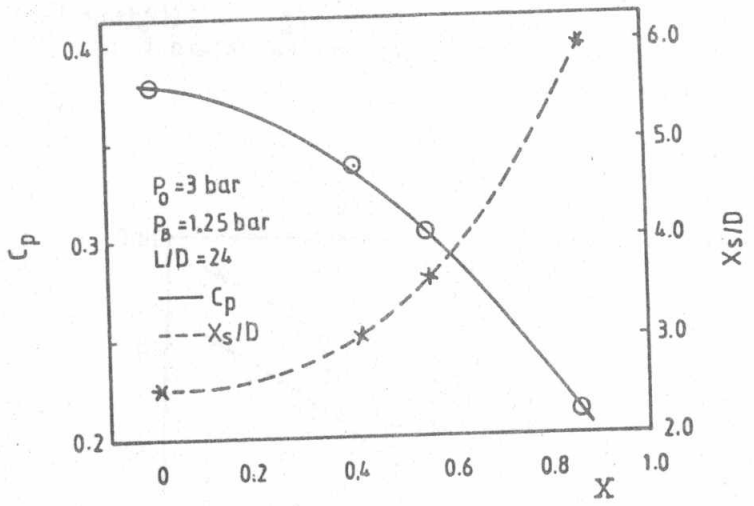

Fig(8) Effect of solids loading ratio on the interaction characterstics

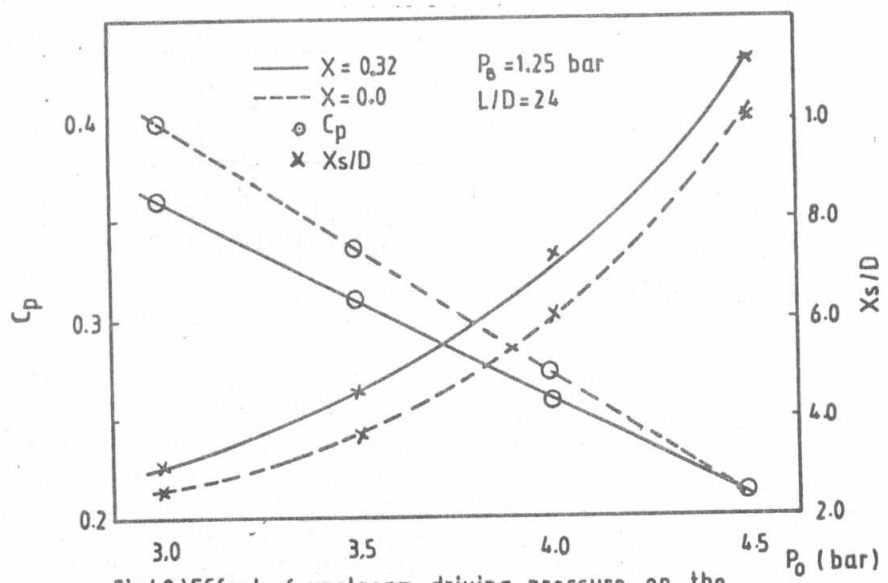

Fig(9) Effect of upstream driving pressure on the interaction characterstics

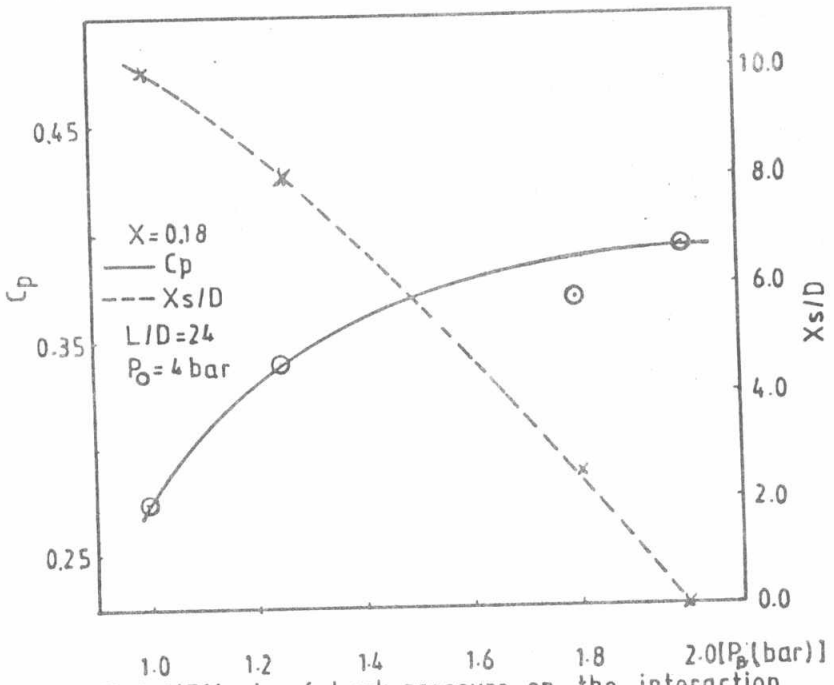

Fig(10)Effect of back pressure on the interaction characteristics.

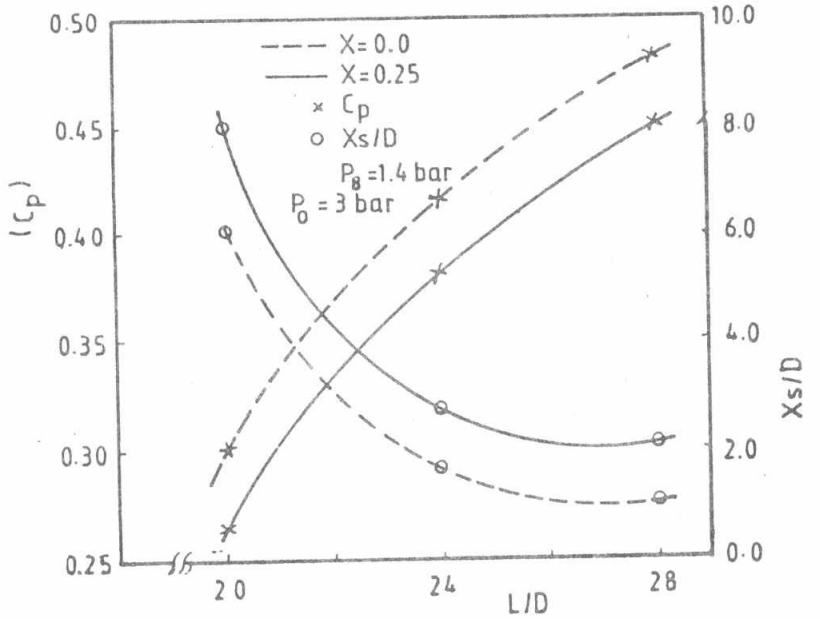

Fig(11)Effect of duct length on the interaction characteristics.

Military Technical College
CAIRO - EGYPT

OUTWARD FLOW BETWEEN A STATIONARY AND A SMALL-ANGLE ROTATING CONICAL -DISK

By

B . A . Khalifa [i] , N .I . I. Hewedy [ii] , M . EL - Kadi [iii]

And A. I . EL - Batran [iv]

ABSTRACT

The flow between a small angle conical rotating disk and a stationary plane disk has been investigated theoretically as well as experimentally in this work . This type of flow has substantial technical applications such that of viscometers , bearings and rotating machines . The present theoretical study deals with numerical solution of the Navier - Stokes equations using the finite difference technique for Newtonian , laminar , incompressible , axisymmetric and steady outward flow with constant properties. Experiments were carried out for different gap heights between the disks , different inlet flow Reynolds numbers and different rotational Reynolds numbers . Comparison between measured pressure distributions in the radial direction and that obtained from the theoretical solution of Navier - Stokes equations as well as the results obtained by analytical solution method developed by others are done . The agreement between measurments and the results obtained from the finite difference method is good for large gaps , large inlet Reynolds numbers and small rotational Reynolds numbers . On the other hand the agreement is better between measurments and the results of analytical solution for small gaps , small inlet Reynolds numbers for all measured values of rotational Reynolds numbers. The study is done for ranges of inlet gap heights non-dimensionalized by the flow inlet diameter of ($0.05 \leq (H=h/Di) \leq 1.0$), inlet flow Reynolds numbers based upon the inlet velocity and inlet diameter ($0.636E+4 \leq (Re_i = \rho Ui\ Di/\mu) \leq 0.318E+5$) and rotational Reynolds numbers ($0.29E+6 \leq (Re_t = \rho \Omega R^2/\mu) \leq 0.123E+7$) for cone angle of about one degree . The result presented here represents a part of results obtained in the M.S.C. [5] .

---

i) Prof , ii) Ass. Prof ,iii) Lecturer , iv) Graduate student , Mechanical Power Engineering Department, Faculty of Engineering & Technology , Menoufia University , Egypt .

INTRODUCTION

The problem of fluid outward flow between a stationary flat disk and a rotating cone disk has many applications in engineering . Some of works dealing with this problem are reviewed here . In [2] the flow between a shallow rotating cone and stationary plate has been investigated visually . Moreover, measurements of the torque required to rotate the conical disk were conducted . An expansion of the Navier-Stokes equations is performed for small values of the single parameter ($Re_c.\alpha^2/12$) . There were agreements between theoretical and the measured results in the range of ($0.5 \leq (Re_c.\alpha^2/12) \leq 4$) .

In [7] the laminar outward flow in a narrow gap between two disks rotating with angular velocities Ω1 and Ω2 is considered. The effect of symmetrical convergent gaps of inlet to outlet height ratios (B2/B1) from 0.25 to 1.0 have been studied , by solving the simplified Navier - Stokes equations using finite differences method .

In this work theoretical and experimental studies are presented for incompressible fluid flow between a stationary and a rotating conical disk with small angle (of about one degree). The problem to be solved is sketched in Fig.(1) , (h) is the minimum gap height between the stationary and the rotating cone disk and the variable gap has the height (hr). The fluid enters the domain axially through a circular opening of diameter (Di) in the stationary one,the outer diameter of the rotating disk is (Do) and the angle of the rotating cone is (α) . A parabolic velocity profile (Ui) is assumed at the inlet .

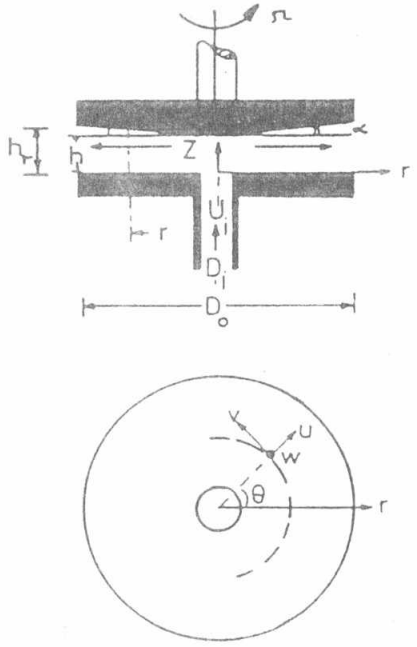

Fig.1
Flow between a stationary and rotating conical disk

THE GOVERNING EQUATIONS

A laminar, outward, axisymmetric and steady flow in the gap is considered . The fluid is assumed to be incompressible and of constant properties . The gap height is an arbitrary function of radius . The last assumptions were used in [4] . Under these assumptions the Navier - stokes equations describing the flow between a stationary and rotating cone disk can be written in the following form (see Fig.(1)) .

Continuity Equation:

$$(1/r)\partial(ru)/\partial r + \partial w/\partial z = 0 \qquad (1)$$

r - Momentum Equation :

$$\rho\left[u\frac{\partial u}{\partial r} - \frac{v^2}{r} + w\frac{\partial u}{\partial z}\right] = -\frac{\partial p}{\partial r} + \mu\left[\frac{\partial}{\partial r}\left(\frac{1}{r}\frac{\partial}{\partial r}(ru)\right) + \frac{\partial^2 u}{\partial z^2}\right] \qquad (2)$$

θ - Momentum Equation :

$$\rho\left[u\frac{\partial v}{\partial r} + \frac{uv}{r} + w\frac{\partial v}{\partial z}\right] = \mu\left[\frac{\partial}{\partial r}\left(\frac{1}{r}\frac{\partial}{\partial r}(rv)\right) + \frac{\partial^2 v}{\partial z^2}\right] \qquad (3)$$

z - Momentum Equation

$$\rho\left[u\frac{\partial w}{\partial r} + w\frac{\partial w}{\partial z}\right] = -\frac{\partial p}{\partial z} + \mu\left[\frac{1}{r}\frac{\partial}{\partial r}\left(r\frac{\partial w}{\partial r}\right) + \frac{\partial^2 w}{\partial z^2}\right] \qquad (4)$$

METHOD OF SOLUTION

Equations (1) to (4) were solved by the SIMPLE algorithm of Smith [3] by applying the finite difference procedure . The velocity components are determined by the solution of their discretization equations and the pressure is calculated depending on the computed fluid flow field . A (15 x 11) grid is applied with 15 grid lines parallel to z - direction and 11 grid lines parallel to the radial direction , see Fig.2 . An

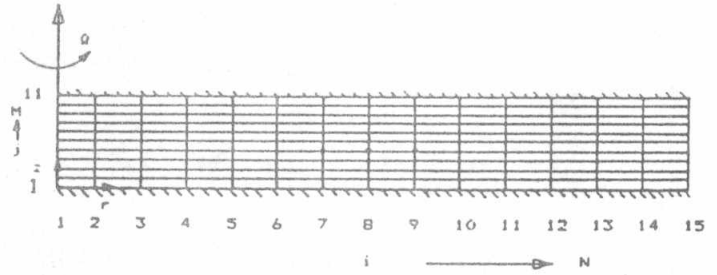

Fig.2 The used grid spacing .

explicit method of solution was used in the calculations because of its simplecity , using a very small axial step Δz whilethe process is valid only for $0 < (\Delta z/\Delta r) \leq 0.5$ and Δr must be kept small in order to attain reasonable accuracy [3] . To solve the equations by this technique the following boundary conditions were used :

At $z = 0$; $Di/2 \leq r \leq Do/2$: $u = v = w = 0$ (5)

At $z = h$; $0 \leq r \leq Do/2$: $u = w = 0$ & $v = \Omega r$ (6)

The initial conditions at the inlet section were taken as :

$p(z) = \text{const}$. (7)

The initial velocity profiles $u(z)$, $v(z)$ and $w(z)$ are taken from [5] as :

$u(z) = (3Q/\pi rh)(zh - z^2)$, $v(z) = \Omega rz/h$ and $w(z) = 0$ (8)

For every internal grid point ($1 < j < N$) , ($1 < i < N$) , Eqns.(1) to (4) are replaced by the algebraic finite-difference approximations using forward - finite difference formula for the first derivatives and centeral-difference formulas for the second derivatives . After appling the last approximations on momentum and continuity equations , it gives a formula for the unknown velocities $u_{i+1,j}$, $v_{i+1,j}$ and $w_{i+1,j}$ and pressure $p_{i+1,j}$ at the (i+1,j)th mesh point in term of known velocities and pressure along the j-th column . The equations of these variables are given in [5] as follow :

$$u_{i+1,j} = u_{i,j} - A_1(\Delta r/r) - w_{i,j+1}(\Delta r/\Delta z) + w_{i,j}(\Delta r/\Delta z) \quad (9)$$

$$v_{i+1,j} = (B/A)v_{i,j+1} + (C/A)v_{i,j-1} + (D/A)v_{i,j} + (E/A)v_{i-1,j} - (A_1B_1/r) - \mu B_1/\rho r^2 \quad (10)$$

$$w_{i+1,j} = (B/A)w_{i,j+1} + (C/A)w_{i,j-1} + (D/A)w_{i,j} + (E/A)w_{i-1,j} + (1/\rho)(p_{i,j} - p_{i,j+1}) \quad (11)$$

$$p_{i+1,j} = p_{i,j} - (AF)u_{i+1,j} + (BF)u_{i,j+1} + (CF)u_{i,j-1} + (DF)u_{i,j} + Eu_{i-1,j} - A_1/r^2 + B^2{}_1/r \quad (12)$$

where A_1, B_1 and C_1 are the radial, tangential and axial velocities at the inlet respectively and A, B, C, D, E and F are given by:

$$\begin{aligned} A &= A_1/\Delta r - (\mu/\rho\Delta r^2) - (\mu/\rho r\Delta r), \\ B &= (\mu/\Delta z^2) - (C_1/\Delta z), \\ C &= (\mu/\rho z^2), \\ D &= A_1/\Delta r + C_1/\Delta z - (2\mu/\rho\Delta r^2) - (\mu/\rho r\Delta r) - (2\mu/\Delta z^2), \\ E &= \mu/\rho\Delta r^2 \text{ and} \\ F &= \rho\Delta r \end{aligned} \quad (13)$$

Hence one can calculate the unknown pivotal values of u along the first i- column in terms of known boundary and initial values at i=1 . Then the unknown pivotal values along the second i- column can be determined from the calculated pivotal values , this steps are executed for the other parameters of flow . At every step the pressure at the (i+1,j)th was calculated . A computer program is executed to solve the last equations to find the pressure distributions . A flow chart represents the steps of solution of this computer program are given in [5] .

SOME EXPERIMENTAL DETAILS

A testing apparatus is designed to carry out the experimental work of this investigation . The apparatus is shown in Fig.(3). The principal object of this work was to determine the radial pressure distribution between the disks , which were obtained from a bank of manometers coupled to static pressure tapings seperated by 5 mm radial distances betweeen each others in the stationary disk .The test apparatus consists of face plate,back plate,cylinderical housing,stationary disk and a rotating disk, with small cone angle of about one degree . All the last parts were made of presspex , the other parts which formed the apparatus as the driving , suppply circuit and the measuring devices are made from other materials . Complete describtion of the apparatus are given in [5] .

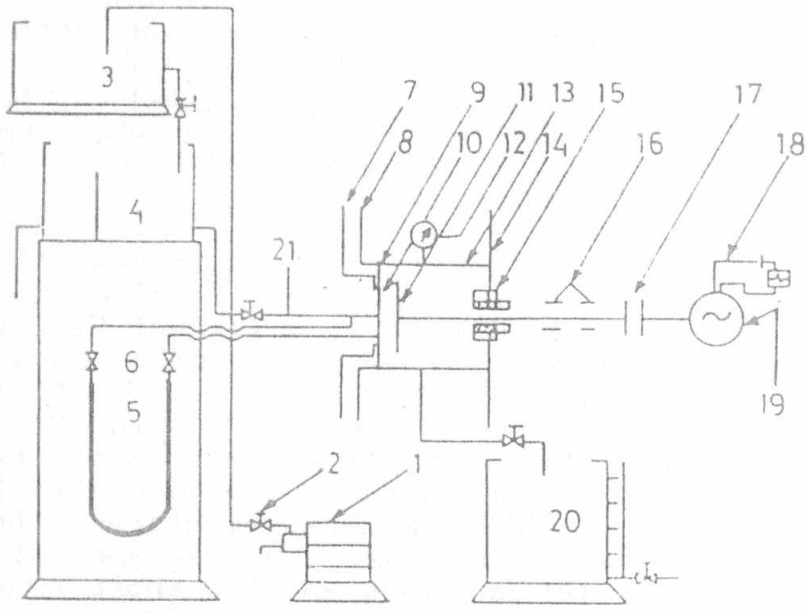

(1) Electric pump
(2) Gate valve
(3) Main tank
(4) over flow tank
(5) Manometer
(6) Ventilation valve
(7) Adjusting head
(8) Front plate
(9) O-ring
(10) Stationary disk
(11) Rotating disk
(12) Borden gauge
(13) Cylinder
(14) Bake plate
(15) Stuffing box
(16) Bearing
(17) Flexible coupling
(18) Electric circuit
(19) Electric motor
(20) Collecting tank
(21) inlet tube

Fig.3 Schematic diagram of the experimental set up .

THE EXPERIMENTAL RESULTS :

This section is concerned with the discussion of the experimental measurements . The measurements of radial pressure are represented in Fig.(4) . Figs.4(a,b) show the effect of varying the rotational Reynolds number on the radial pressure distribution at H=0.1 and H=1.0 . Increasing the rotational Reynolds number leads to increase in negative pressure . All the curves take the same trend and the maximum negative pressure is shown at a radius ratio of about $\bar{R} = 5.0$. This result is refered to increasing the hydraulic losses in the entrance region of the disk and the vena-contracta effect . The same result can be shown in Fig.4(c) which profiled the effect of varying the gap height on the radial pressure distribution at constant inlet and rotational Reynolds numbers . Increasing the gap height results decreasing of minimum pressure .

Introducing the effect of one degree cone angle on the radial pressure distribution in comparison with the results of flat disk (obtained from [5]) is shown in Fig.4(d) at different values of H . The pressure distribution for the flat disk is presented by the curves of number (1) and for the conical disk by (2) . The cone angle increases the amplitude of the negative pressure at small H ,while at higher H ,H = 1 the value of maximum pressure drop is reduced .

COMPARISON BETWEEN MEASURMENTS AND THEORIES:

This section concerns with the comparison between the experimental and the theoretical results obtained from both of the analytical method of simplified Navier - Stokes equations obtained from [6] and that obtained from the solution of the Navier-Stokes equations by the finite difference method (FDM) which is given in this work . The inertia of flow terms are included in the last solution while it was not included in the analytical method . So some experimental pressure profiles are represented with the theoretical results in the two cases of solution at same initial and boundary conditions .

Fig.(5) represents the pressure measurements as well as the computed pressure distributions obtained from analytical method (AM) and the finite difference method (FDM) at different values of H , Re_i and Re_t for flow between a stationary flat disk and an rotating cone disk of about one degree cone angle . Fig.5(a) shows the results for H=0.05 , Fig.5(b) for H=0.1 and Figs.5(c) and 5(d) for H=0.3 and 1.0 respectively . It is clear from the results that there are large deviations between the theoretical results obtained from both methods and the measurements at the inlet region . These deviations could be explained as a result of the place of measuring the inlet pressure and the sharp edge effect at the inlet , in which the flow changes it's direction from axial to radial direction causing a small seperation region.These effects are concluded in the measurements but were neglected in the theoretical analysis . The agreement between the measured pressure distributions and the theoretical results

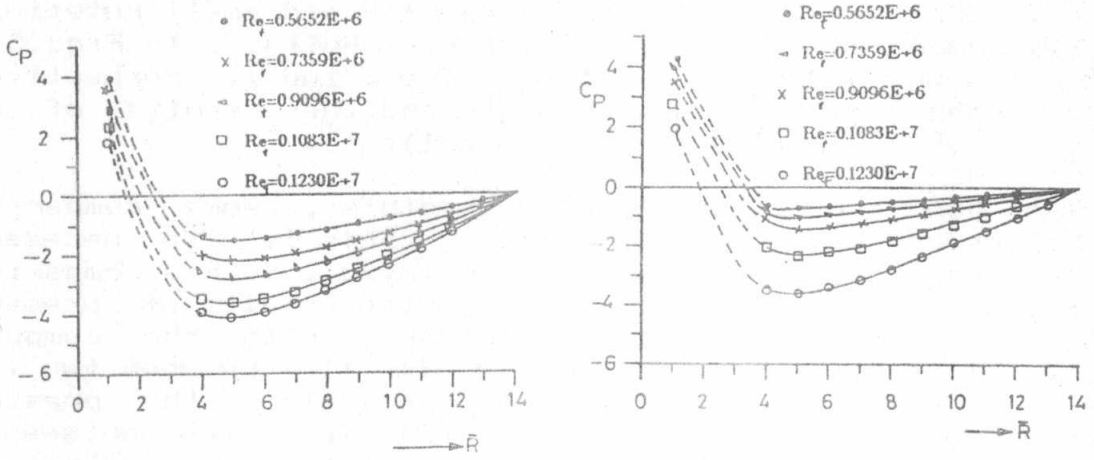

(a) Re_i=0.318E+5, H=0.10 (b) Re_i=0.318E+5, H=1.0

Effect of rotational Reynolds number

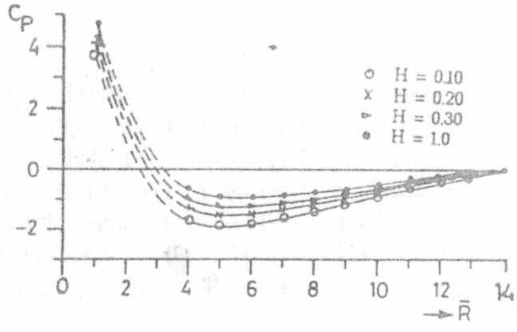

(c) Effect of gap height
Re_i=0.32E+5 , Re_t=0.74E+6

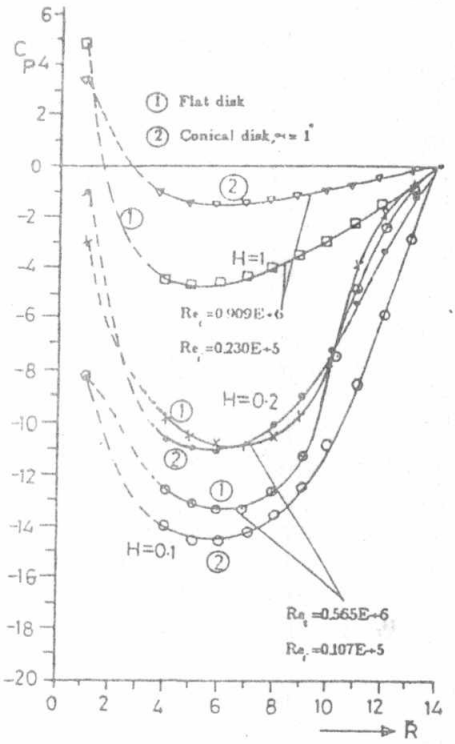

(d) Comparison between flat and conical disk

Fig.4. Experimental pressure distributions

from the analytical method (AM) at small value of gap height H, (H=0.05) for given range of Re_i and Re_t is excellent, Fig.5(a) . In Fig.5(b), where H=0.1, the agreement between measured and computed results obtained from the finite difference method is good for given values of the inlet and rotational Reynolds number . That means a greater values of H and small rotational Reynolds number the (FDM) gives better results . In Figs.5(c) and 5(d) in which H has the values of 0.3 and 1.0 respectively the agreement between measurements and the results of the finite difference method (FDM) is excellent .

For the numerical solution to be credible , some comparison with others computaions is essential . This is also necessery to ensure the edequacy of the grid employed . Such a comparison is presented in Fig.5(e) . The computed results of pressure distributions in this work are compared with the computed results of Prakash and coworkers [4] for flow between two flat disks (1) . To show the effect of cone angle on the pressure distribution , the results of (FDM) for flow between a stationary flat- and a rotating conical plate (cone angle ≈ 1) are also presented in Fig.5(e) by curves (2) . The computation results presented from [4] are presented only for flow between two flat disks ,(dotted lines) . The comparisons are done for two values of inlet Reynolds number (Re_i= 100 & 1000) , but for the same gap height ,(H = 0.5) and rotational Reynolds number , (Re_t = 100) . The agreement between both computations for the flow type (1) is good at the given two inlet Reynolds numbers , (Re_i= 100 & 1000) . The deviation between the computations for the flow type (2) at Re_i= 100 is due to the cone angle . As can be seen the agreement between the computed results of this work and that in [4] for flow between two flat disks is quite satisfactory .

CONCLUSIONS :

From the results obtained from this work the following conclusions are drawn :

1. The analytical method (AM) gives a good agreement with the experimental results for the big rotational Reynolds numbers ,small inlet Reynolds numbers and small gap heights . This agreement could be explained as an effect of the big value of inertia due to rotation and small value of inertia due to flow . The deviation increases at big gaps and at high inlet Reynols numbers,at which the flow inertia has big values .

2. The increase of the rotational Reynolds number increases the amplitude of pressure and this depends upon the inlet Reynolds number and the outer radius of the rotating disk also .

3. The increase in the gap height increases the inertia of the flow , so the pressure will increase by increasing the gap height and this increament rate of pressure is smaller at bigger values of gap .

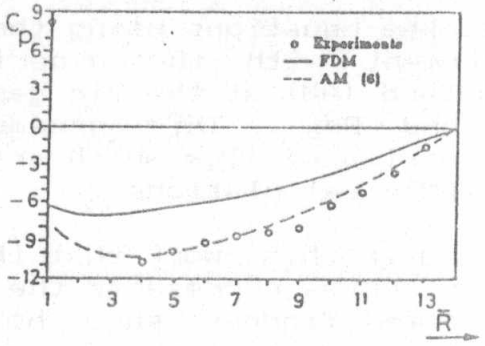

(a)

Re_i=0.69E+4, Re_t=0.35E+6

H= 0.05

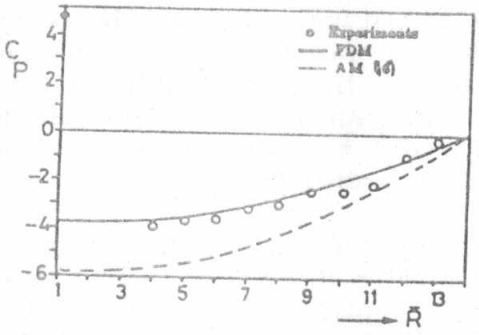

(b)

Re_i=0.94E+4, Re_t=0.35E+6

H=0.1

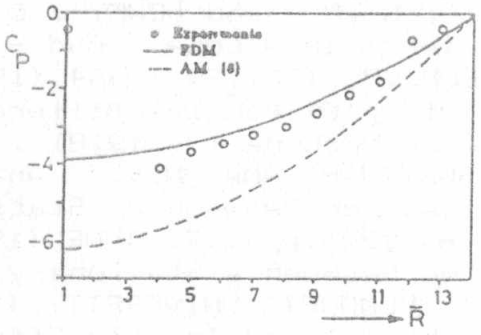

(c)

Re_i=0.94E+4, Re_t=0.35E+6

H=0.3

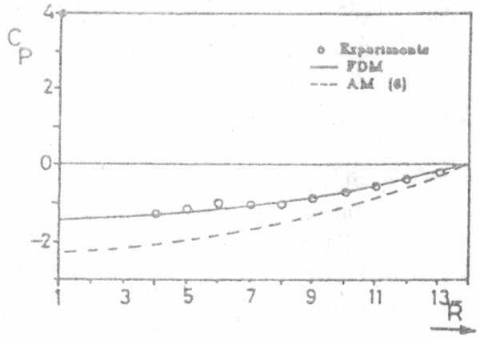

(d)

Re_i=0.25E+5, Re_t=0.56E+6

H=1.0

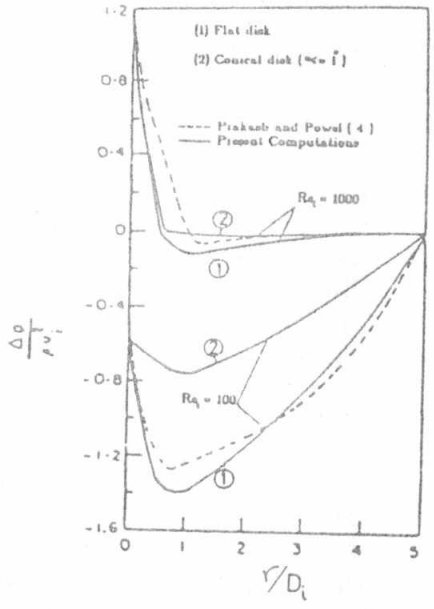

(e)

Comparison between present and other computations at H = 0.5 , Re_t =100

Fig.5. Comparison with experimental and other computational results .

4. The solution of the Navier-stokes equations using the (FDM) gives good and better agreement with the experimental results than the analytical method (AM) at the big gaps, for all measured values of Re_i and Re_ω . This agreement is retained to the terms of the inertia of flow which are taken in the consideration in the (FDM)- calculations .

5. Finally the most important thing in this work that the area under the pressure distribution curves represents the axial thrust upon the disks . Then these figures show how this important parameter is under the control of the designer, by changing the values of H , Re_i and Re_ω.

REFERENCES

1. WARREN , R .B .B ,EDWIN . E . S & LIGHTFOOT.L ''Transport Phenomena'',John Wiley, (1960).
2. SDOUGOS ,H . P ., BUSSOLARI , S .R . and DEWEY , C . F . '' Secondary Flow And Turbulence In A Cone - And - Plate Device.''JOURNAL OF FLUID MECH,VOL.138,379 - 404 (1984) .
3. SMITH ,G .D.'' Numerical Solution Of Partial Differential Equation (Finite Difference Methods) ,(1978) .
4. PRAKASH, C.,POWLE, U.S.and SURYANARAYANA, N.V.'' Analysis of Laminar Flow and Heat Transfer Between a Stationary and a Rotating Disk''AIAA J,84-1806,pp 1-9, JUNE (1984) .
5. El-BATRAN ,A .I .'' Fluid flow Between a Stationary and a Rotating Disk '',M.Sc.Thesis ,MENOUFIA UNIVERSITY,(1988).
6. SALEM, E.A.and KHALIL, F. ''Thermal and Inertia Effect in Externally Pressurized Conical Oil Bearing ''Bull Of Mech Power Eng ., Faculty of Eng ,Alex Uni,Vol xv ,(1976) .
7 PAKULA ,G . and RDUCH,J.'' Laminar Outward Flow In a Gap Between Rotating Disks '',Proceeding of the Eighth Confe- rence on Fluid Machinery,Vol 2,Budapest,15-19 Sept(1987).

NOMENCLATURE

C_p cofficient of pressure = $(p_r - p_R) / 0.5\, \rho\, Ui^2$
Di diameter of the inlet opening = 2Ri
Do outer diameter of the rotating disk = 2R
H dimensionless inlet axial gap height = (h /Di)
h gap height between disks at inlet
hr gap height at any radius
p_r ,p_R pressure at any radius and exit respectivelly
R Radius ratio = r/Ri
Re_i inlet Reynolds number = $\rho\, Ui\, Di / \mu$
Re_ω rotational Reynolds number = $\rho\, \Omega\, R^2 / \mu$
r,θ,z radial -, angular - , & axial coordinats,Fig.1
u,v,w radial -, tangential- ,& axial velocity ,Fig.1
Ui average velocity of the incoming fluid
α angle of the rotating conical disk , Fig.1
ρ density
Ω angular velocity of rotating disk
μ dynamic viscosity .